

Dedicated to the memory of Richard Edward Taylor (1929-2018)

# Measurement of the Nucleon $F_2^n/F_2^p$ Structure Function Ratio by the Jefferson Lab MARATHON Tritium/Helium-3 Deep Inelastic Scattering Experiment

D. Abrams,<sup>1</sup> H. Albataineh,<sup>2</sup> B. S. Aljawrneh,<sup>3</sup> S. Alsalmi,<sup>4,5</sup> K. Aniol,<sup>7</sup> W. Armstrong,<sup>8</sup> J. Arrington,<sup>8,9</sup> H. Atac,<sup>10</sup> T. Averett,<sup>11</sup> C. Ayerbe Gayoso,<sup>11</sup> X. Bai,<sup>1</sup> J. Bane,<sup>12</sup> S. Barcus,<sup>11</sup> A. Beck,<sup>13</sup> V. Bellini,<sup>14</sup> H. Bhatt,<sup>15</sup> D. Bhetuwal,<sup>15</sup> D. Biswas,<sup>16</sup> D. Blyth,<sup>8</sup> W. Boeglin,<sup>17</sup> D. Bulumulla,<sup>18</sup> J. Butler,<sup>19</sup> A. Camsonne,<sup>19</sup> M. Carmignotto,<sup>19</sup> J. Castellanos,<sup>17</sup> J.-P. Chen,<sup>19</sup> E. O. Cohen,<sup>20</sup> S. Covrig,<sup>19</sup> K. Craycraft,<sup>11</sup> R. Cruz-Torres,<sup>13</sup> B. Dongwi,<sup>14</sup> B. Duran,<sup>10</sup> D. Dutta,<sup>15</sup> E. Fuchey,<sup>21</sup> C. Gal,<sup>1</sup> T. N. Gautam,<sup>16</sup> S. Gilad,<sup>13</sup> K. Gnanvo,<sup>1</sup> T. Gogami,<sup>22</sup> J. Gomez,<sup>19</sup> C. Gu,<sup>1</sup> A. Habarakada,<sup>16</sup> T. Hague,<sup>4</sup> J.-O. Hansen,<sup>19</sup> M. Hattawy,<sup>8</sup> F. Hauenstein,<sup>18</sup> D. W. Higinbotham,<sup>19</sup> R. J. Holt,<sup>8</sup> E. W. Hughes,<sup>23</sup> C. Hyde,<sup>18</sup> H. Ibrahim,<sup>24</sup> S. Jian,<sup>1</sup> S. Joosten,<sup>10</sup> A. Karki,<sup>15</sup> B. Karki,<sup>25</sup> A. T. Katramatou,<sup>4</sup> C. Keith,<sup>19</sup> C. Keppel,<sup>19</sup> M. Khachatryan,<sup>18</sup> V. Khachatryan,<sup>26</sup> A. Khanal,<sup>17</sup> A. Kievsky,<sup>27</sup> D. King,<sup>28</sup> P. M. King,<sup>25</sup> I. Korover,<sup>29</sup> S. A. Kulagin,<sup>30</sup> K. S. Kumar,<sup>26</sup> T. Kutz,<sup>26</sup> N. Lashley-Colthirst,<sup>16</sup> S. Li,<sup>31</sup> W. Li,<sup>32</sup> H. Liu,<sup>23</sup> S. Liuti,<sup>1</sup> N. Liyanage,<sup>1</sup> P. Markowitz,<sup>17</sup> R. E. McClellan,<sup>19</sup> D. Meekins,<sup>19</sup> S. Mey-Tal Beck,<sup>13</sup> Z.-E. Meziani,<sup>10</sup> R. Michaels,<sup>19</sup> M. Mihovilovic,<sup>33,34,35</sup> V. Nelyubin,<sup>1</sup> D. Nguyen,<sup>1</sup> Nuruzzaman,<sup>42</sup> M. Nycz,<sup>4</sup> R. Obrecht,<sup>21</sup> M. Olson,<sup>36</sup> V. F. Owen,<sup>11</sup> E. Pace,<sup>37</sup> B. Pandey,<sup>16</sup> V. Pandey,<sup>38</sup> M. Paolone,<sup>10</sup> A. Papadopoulou,<sup>13</sup> S. Park,<sup>26</sup> S. Paul,<sup>11</sup> G. G. Petratos,<sup>4</sup> R. Petti,<sup>39</sup> E. Piasetzky,<sup>20</sup> R. Pomatsalyuk,<sup>40</sup> S. Premathilake,<sup>1</sup> A. J. R. Puckett,<sup>21</sup> V. Punjabi,<sup>41</sup> R. D. Ransome,<sup>42</sup> M. N. H. Rashad,<sup>18</sup> P. E. Reimer,<sup>8</sup> S. Riordan,<sup>8</sup> J. Roche,<sup>25</sup> G. Salmè,<sup>43</sup> N. Santiesteban,<sup>31</sup> B. Sawatzky,<sup>19</sup> S. Scopetta,<sup>44</sup> A. Schmidt,<sup>13</sup> B. Schmookler,<sup>13</sup> J. Segal,<sup>19</sup> E. P. Segarra,<sup>13</sup> A. Shahinyan,<sup>45</sup> S. Širca,<sup>33,34</sup> N. Sparveris,<sup>10</sup> T. Su,<sup>4,46</sup> R. Suleiman,<sup>19</sup> H. Szumila-Vance,<sup>19</sup> A. S. Tadepalli,<sup>42</sup> L. Tang,<sup>16,19</sup> W. Tireman,<sup>47</sup> F. Tortorici,<sup>14</sup> G. M. Urciuoli,<sup>48</sup> B. Wojtsekhowski,<sup>19</sup> S. Wood,<sup>19</sup> Z. H. Ye,<sup>8\*</sup> Z. Y. Ye,<sup>49</sup> and J. Zhang<sup>26</sup>

<sup>1</sup>University of Virginia, Charlottesville, VA 22904, USA

<sup>2</sup>Texas A & M University, Kingsville, TX 78363, USA

<sup>3</sup>North Carolina A & T State University, Greensboro, NC 27411, USA

<sup>4</sup>Kent State University, Kent, OH 44240, USA

<sup>5</sup>King Saud University, Riyadh 11451, Kingdom of Saudi Arabia

<sup>6</sup>University of Zagreb, 10000 Zagreb, Croatia

<sup>7</sup>California State University, Los Angeles, CA 90032, USA

<sup>8</sup>Argonne National Laboratory, Lemont, IL 60439, USA

<sup>9</sup>Lawrence Berkeley National Laboratory, Berkeley, CA 94720, USA

<sup>10</sup>Temple University, Philadelphia, PA 19122, USA

<sup>11</sup>William & Mary, Williamsburg, VA 23187, USA

<sup>12</sup>University of Tennessee, Knoxville, TN 37996, USA

<sup>13</sup>Massachusetts Institute of Technology, Cambridge, MA 02139, USA

<sup>14</sup>Istituto Nazionale di Fisica Nucleare, Sezione di Catania, 95123 Catania, Italy

<sup>15</sup>Mississippi State University, Mississippi State, MS 39762, USA

<sup>16</sup>Hampton University, Hampton, VA 23669, USA

<sup>17</sup>Florida International University, Miami, FL 33199, USA

<sup>18</sup>Old Dominion University, Norfolk, VA 23529, USA

<sup>19</sup>Jefferson Lab, Newport News, VA 23606, USA

<sup>20</sup>School of Physics and Astronomy, Tel Aviv University, Tel Aviv, Israel

<sup>21</sup>University of Connecticut, Storrs, CT 06269, USA

<sup>22</sup>Tohoku University, Sendai 980-8576, Japan

<sup>23</sup>Columbia University, New York, NY 10027, USA

<sup>24</sup>Cairo University, Cairo, Giza 12613 Egypt

<sup>25</sup>Ohio University, Athens, OH 45701, USA

<sup>26</sup>Stony Brook, State University of New York, NY 11794, USA

<sup>27</sup>Istituto Nazionale di Fisica Nucleare, Sezione di Pisa, 56127 Pisa, Italy

<sup>28</sup>Syracuse University, Syracuse, NY 13244, USA

<sup>29</sup>Nuclear Research Center-Negev, Beer-Sheva 84190, Israel

<sup>30</sup>Institute for Nuclear Research of the Russian Academy of Sciences, 117312 Moscow, Russia

<sup>31</sup>University of New Hampshire, Durham, NH 03824, USA

<sup>32</sup>University of Regina, Regina, SK S4S 0A2, Canada

<sup>33</sup>Faculty of Mathematics and Physics, University of Ljubljana, Ljubljana 1000, Slovenia

<sup>34</sup>Jožef Stefan Institute, Ljubljana, Slovenia

<sup>35</sup>Institut für Kernphysik, Johannes Gutenberg-Universität, Mainz 55122, Germany

<sup>36</sup>Saint Norbert College, De Pere, WI 54115, USA

<sup>37</sup>University of Rome Tor Vergata and INFN, Sezione di Roma Tor Vergata, 00133 Rome, Italy

<sup>38</sup>Center for Neutrino Physics, Virginia Tech, Blacksburg, VA 24061, USA

<sup>39</sup>University of South Carolina, Columbia, SC 29208, USA

<sup>40</sup>Institute of Physics and Technology, 61108 Kharkov, Ukraine

<sup>41</sup>Norfolk State University, Norfolk, VA 23504, USA

<sup>42</sup>Rutgers, The State University of New Jersey, Piscataway, NJ 08855, USA

<sup>43</sup>Istituto Nazionale di Fisica Nucleare, Sezione di Roma, 00185 Rome, Italy

<sup>44</sup>University of Perugia and INFN, Sezione di Perugia, 06123 Perugia, Italy

<sup>45</sup>Yerevan Physics Institute, Yerevan 375036, Armenia

<sup>46</sup>Shandong Institute of Advanced Technology, Jinan, Shandong 250100, China

<sup>47</sup>Northern Michigan University, Marquette, MI 49855, USA

<sup>48</sup>Istituto Nazionale di Fisica Nucleare, Sezione di Roma, 00185 Rome, Italy and

<sup>49</sup>University of Illinois-Chicago, Chicago, IL 60607, USA

(Dated: April 14, 2021)

The Jefferson Lab Hall A Tritium Collaboration

Submitted to *Physical Review Letters*

The ratio of the nucleon  $F_2$  structure functions,  $F_2^n/F_2^p$ , is determined by the MARATHON experiment from measurements of deep inelastic scattering of electrons from  $^3\text{H}$  and  $^3\text{He}$  nuclei. The experiment was performed in the Hall A Facility of Jefferson Lab and used two high resolution spectrometers for electron detection, and a cryogenic target system which included a low-activity tritium cell. The data analysis used a novel technique exploiting the mirror symmetry of the two nuclei, which essentially eliminates many theoretical uncertainties in the extraction of the ratio. The results, which cover the Bjorken scaling variable range  $0.19 < x < 0.83$ , represent a significant improvement compared to previous SLAC and Jefferson Lab measurements for the ratio. They are compared to recent theoretical calculations and empirical determinations of the  $F_2^n/F_2^p$  ratio.

PACS numbers: 12.38.-7, 13.60.-r, 14.65.-q, 25.30.-c, 27.10.+h

The nucleon structure functions, found from deep inelastic scattering (DIS) of electrons by protons and deuterons, have been of fundamental importance in establishing the internal quark structure of the nucleon [1]. First measurements occurred in a series of DIS experiments at the Stanford Linear Accelerator Center (SLAC) circa 1970 [2], which showed the existence of point-like entities within the nucleons. Further studies of muon-nucleon and neutrino-nucleon DIS experiments at CERN and Fermilab [3] established the quark-parton model (QPM) for the nucleon [4], and provided supporting evidence for the emerging theory of quantum chromodynamics (QCD) [5].

The cross section for deep inelastic electron-nucleon scattering, where the nucleon breaks up, is given, in the one-photon-exchange approximation, in terms of the structure functions  $F_1(\nu, Q^2)$  and  $F_2(\nu, Q^2)$  of the nucleon. In the lab frame and in natural units it reads [4]:

$$\frac{d^2\sigma}{d\Omega dE'} = \sigma_M \left[ \frac{F_2(\nu, Q^2)}{\nu} + \frac{2F_1(\nu, Q^2)}{M} \tan^2 \left( \frac{\theta}{2} \right) \right], \quad (1)$$

where  $\sigma_M = \frac{4\alpha^2(E')^2}{Q^4} \cos^2 \left( \frac{\theta}{2} \right)$  is the Mott cross section,  $\alpha$  is the fine-structure constant,  $E$  is the incident electron energy,  $E'$  and  $\theta$  are the scattered elec-

tron energy and angle,  $\nu = E - E'$  is the energy transfer,  $Q^2 = 4EE' \sin^2(\theta/2)$  is the negative of the four-momentum transfer squared, and  $M$  is the nucleon mass.

The scattering process is mediated through the exchange of virtual photons. The cross section can also be written in terms of cross sections for the absorption by the nucleon of longitudinally,  $\sigma_L$ , or transversely,  $\sigma_T$ , polarized photons. The functions  $F_1$  and  $F_2$  are related to the ratio  $R = \sigma_L/\sigma_T$  as  $F_1 = MF_2(\nu^2 + Q^2)/[Q^2\nu(1 + R)]$  [2]. All of the above formalism can also be applied to the case of DIS by a nucleus, with  $F_1$  and  $F_2$  becoming the structure functions of the nucleus in question. It should be noted that the ratio of DIS cross sections of different nuclear targets is equivalent to the ratio of their  $F_2$  structure functions if  $R$  is the same for all nuclei. The latter has been confirmed experimentally within inherent experimental uncertainties [6].

The basic idea of the QPM [7, 8] is to represent DIS as quasi-free scattering of electrons from the nucleon's partons/quarks, in a frame where the nucleon possesses infinite momentum. The fractional momentum of the nucleon carried by the struck quark is then given by the Bjorken “scaling” variable,  $x = Q^2/(2M\nu)$ . In the limit where  $\nu \rightarrow \infty$ ,  $Q^2 \rightarrow \infty$  with  $x$  finite between 0 and 1, the nucleon structure functions become:  $F_1 = \frac{1}{2} \sum_i e_i^2 f_i(x)$  and  $F_2 = x \sum_i e_i^2 f_i(x)$ , where  $e_i$  is the fractional charge of quark type  $i$ ,  $f_i(x)dx$  is the probability that a quark of type  $i$  carries momentum in the range between  $x$  and  $x + dx$ , and the sum runs over all

---

\*Present address: Canon Medical Research USA Inc., Vernon Hills, IL 60061

quark types. Since the charges of the up ( $u$ ), down ( $d$ ) and strange ( $s$ ) quarks are  $2/3$ ,  $-1/3$  and  $-1/3$ , respectively, the  $F_2(x)$  structure function for the proton ( $p$ ) is given by:  $F_2^p(x) = x[(4/9)U + (1/9)D + (1/9)S]$ , and due to isospin symmetry, that of the neutron ( $n$ ) is given by:  $F_2^n(x) = x[(1/9)U + (4/9)D + (1/9)S]$ , where  $U = u + \bar{u}$ ,  $D = d + \bar{d}$ , and  $S = s + \bar{s}$ , with bars denoting antiquarks [4].

The positivity of the structure functions dictates that the ratio of the neutron to proton  $F_2$  functions is bounded for all values of  $x$ :  $(1/4) \leq F_2^n/F_2^p \leq 4$ , a relationship known as the Nachtmann inequality [9]. This relationship was verified in the pioneering SLAC experiments E49a and E49b circa 1970 [10], which found that the ratio approaches unity at  $x = 0$  and  $\sim 1/4$  at  $x = 1$ . The SLAC findings showed that at low  $x$  the three quark-antiquark distributions are equal, dominated by sea quarks, and that at large  $x$  the  $u$  ( $d$ ) quark distribution dominates in the proton (neutron). These findings were surprising as the expectation, at the time, from SU(6) symmetry was that  $F_2^n/F_2^p$  should be equal to  $2/3$  for all  $x$ . The behavior of the ratio at  $x = 1$  was justified by the diquark model of Close [11], and Regge phenomenology, initiated by Feynman [12]. In Close's diquark model, the diquark configuration with spin 1 is suppressed relative to that with spin 0. The phenomenological suppression of the  $d$  quark distribution, which results from the  $F_2^n/F_2^p$  value of  $1/4$  at  $x = 1$ , can be understood in the quark model of Isgur [13] in terms of the color-magnetic hyperfine interaction between quarks, which is also responsible for the  $N$ - $\Delta$  mass splitting. It should be noted that perturbative QCD arguments [14] and a treatment based on quark-counting rules [15] suggest that the nucleon  $F_2$  ratio should have the larger value of  $3/7$  at  $x = 1$ .

The original considerations of the magnitude of the nucleon  $F_2$  ratio were called into question in the 1990s when a re-examination of the subject by Whitlow *et al.* [16], who using the original SLAC data [10] and a plausible model of the EMC effect in which the deuteron, medium and heavy nuclei scale with nuclear density [17], found a strong sensitivity in the determination of the ratio at large  $x$ . The EMC effect, discovered at CERN [18] and quantified precisely at SLAC [19], characterizes the modification of the nucleon structure functions in nuclear matter. The above strong sensitivity was subsequently confirmed by Melnitchouk and Thomas [20], in a relativistic re-analysis of the SLAC data, which assumes the presence of minimal binding effects in the deuteron. In Ref. [16], it also became evident that the nucleon  $F_2$  ratio was very sensitive to the choice of the nucleon-nucleon (N-N) potential model governing the structure of deuterium, later confirmed in Refs. [21, 22]. The large uncertainty in the extraction of the  $F_2^n/F_2^p$  ratio at large  $x$  calls into question the presumption that  $F_2^n/F_2^p$  and  $D/U$  tend to  $1/4$  and zero, respectively, as  $x$  approaches 1.

These difficulties in the  $F_2^n/F_2^p$  determination can be remedied using a method proposed by Afnan *et al.* [23, 24], which determines the  $F_2^n/F_2^p$  ratio from DIS

measurements on  $^3\text{H}$  (triton) and  $^3\text{He}$  (helion), exploiting the isospin symmetry and similarities of the two  $A = 3$  mirror nuclei. In the absence of Coulomb interactions and for an isospin symmetric world, the properties of a proton (neutron) bound in the  $^3\text{He}$  nucleus should be identical to that of a neutron (proton) bound in the  $^3\text{H}$  nucleus. Defining the EMC-type ratios for the  $F_2$  structure functions of helion ( $h$ ) and triton ( $t$ ) by:  $R_h = F_2^h/(2F_2^p + F_2^n)$  and  $R_t = F_2^t/(F_2^p + 2F_2^n)$ , one can write the ratio of these ratios as  $\mathcal{R}_{ht} = R_h/R_t$ , which directly yields the ratio of the free neutron to proton  $F_2$  structure functions:

$$\frac{F_2^n}{F_2^p} = \frac{2\mathcal{R}_{ht} - F_2^h/F_2^t}{2F_2^h/F_2^t - \mathcal{R}_{ht}}. \quad (2)$$

The  $F_2^n/F_2^p$  ratio found from Equation (2) depends on the ratio of the EMC effects in  $^3\text{He}$  and  $^3\text{H}$ . Since the neutron and proton distributions in the  $A = 3$  nuclei are similar, the ratio can be calculated reliably with the expectation that  $\mathcal{R}_{ht} \simeq 1$  [24], once  $F_2^h/F_2^t$  is measured experimentally. The possibility for such a determination, proposed at Jefferson Lab (JLab) in 1999 [25], was also supported by the works of Refs. [26] and [27]. An official JLab proposal (PR12-10-103) [28] was submitted to and approved by the Lab in 2010.

This JLab E12-10-103 experiment, known also as MARATHON [28], used the Continuous Electron Beam Accelerator and Hall A Facilities over 66 days in the winter/spring of 2018. Electrons scattered from light nuclei were detected in the Left and Right High Resolution Spectrometers (LHRS and RHRS) [29]. The incident-beam energy was fixed at 10.59 GeV, and the beam current ranged from 14.6 to 22.5  $\mu\text{A}$ . The experiment detected DIS events from the proton, deuteron, helion, and triton particles using a cryogenic gaseous target system [30]. The LHRS was operated at a fixed momentum of 3.1 GeV/ $c$ , placed at angles between  $16.81^\circ$  and  $33.55^\circ$ . The RHRS was limited in momentum and was, therefore, operated at a single setting of 2.9 GeV/ $c$  and  $36.12^\circ$ .

The target system consisted of four high-pressure cells, of length 25.0 cm and diameter 1.27 cm, containing  $^3\text{He}$ ,  $^3\text{H}$ ,  $^2\text{H}$ , and  $^1\text{H}$  gases. The four cells were filled at temperatures of 294.3, 296.3, 296.1, 297.4 K, and pressures of 17.19, 13.82, 35.02, 35.02 atm, resulting in densities (determined from data-supported virial models [31]) of  $2.129 \pm 0.021$ ,  $3.400 \pm 0.010$ ,  $5.686 \pm 0.022$ , and  $2.832 \pm 0.011 \text{ kg/m}^3$ , respectively. To prevent overheating, the target cells were cooled to a temperature of 40 K, and the beam current was limited to 22.5  $\mu\text{A}$ . The target assembly also contained an empty cell and a "dummy target" consisting of two Al foils separated by 25.0 cm, which were used to measure the contribution to the scattered electron yields from the Al end-caps of the target cells. The targets were cycled many times in the beam for each kinematic setting in order to minimize effects of possible drifts of the beam diagnostic or other instrumentation (*e.g.* the beam current monitors). Because of safety hazards associated with (radioactive) tritium,

$x$	$Q^2$ (GeV/c) <sup>2</sup>	$W^2$ (GeV/c <sup>2</sup> ) <sup>2</sup>	$\sigma_d/\sigma_p$	$\Delta_{\text{stat}}$	$\Delta_{\text{ptp}}$	$\Delta_{\text{syst}}$	$\Delta_{\text{tot}}$
0.195	2.73	12.2	1.725	0.005	0.010	0.009	0.015
0.225	3.15	11.7	1.697	0.005	0.008	0.009	0.014
0.255	3.57	11.3	1.674	0.007	0.008	0.009	0.014
0.285	3.99	10.9	1.656	0.008	0.010	0.009	0.016
0.315	4.41	10.5	1.629	0.008	0.010	0.009	0.016
0.345	4.83	10.1	1.588	0.009	0.010	0.009	0.016
0.375	5.25	9.63	1.544	0.013	0.016	0.008	0.023

TABLE I: The ratio of deuteron to proton DIS cross section at the selected  $x$ ,  $Q^2$ , and  $W^2$  kinematics of MARATHON. Listed are the statistical (stat), point-to-point (ptp), and overall/scale systematic (syst) components of the total (tot) error. The latter is the quadrature sum of the three components. The overall/scale systematic component of  $\pm 0.55\%$  is due to the uncertainties in the nominal gas target densities of the hydrogen and deuterium gases (combined in quadrature).

such targets have been used only twice in past electronuclear physics experiments in the USA (Stanford [32] and MIT [33]).

Scattered electrons were detected in the LHRS and RHRS using two planes of scintillators for event triggering, a pair of drift chambers for electron track reconstruction, and a gas threshold Čerenkov counter and a lead-glass calorimeter for electron identification. The event trigger consisted of a coincidence of the logical signals of either one of the two scintillator planes and the Čerenkov counter, which is estimated to be efficient at the 99% level. Details on the Hall A Facility, and beam line and detector instrumentation as used in MARATHON, including calibrations, are given in Refs. [34–39].

Particles in the two HRS systems were identified as electrons on the basis of a minimal pulse height in the Čerenkov counter (“Čerenkov cut”) and the energy deposited in the calorimeter, consistent with the momentum as determined from the drift chamber track using the spectrometers’ optical properties (“calorimeter cut”). The detector efficiencies for both spectrometers were found to be stable, and independent of the gas target used at a given kinematics. The efficiency of the Čerenkov detectors was above 99% (the average number of photoelectrons for the LHRS and RHRS detectors were 11 and 9, respectively). The efficiency of the preradiator segments of the calorimeters was above 99%, and that of the total absorption segments was above 98%. The FWHM energy resolution of the two calorimeters were measured to be  $5.0\%/\sqrt{E'}$  and  $4.3\%/\sqrt{E'}$  for the LHRS and RHRS, respectively.

Because of the low density of the gas targets, the electron counting rate was dominated, for all kinematics, by events originating from the target cell Al end-caps, as the total thickness of the two end-caps of the  $^3\text{He}$ ,  $^3\text{H}$ ,  $^2\text{H}$  and  $^1\text{H}$  cells was 0.55, 0.60, 0.51, and 0.64 mm, respectively. Tritium-safety concerns prevented the use of collimators to mask the end-caps of the cells from the spectrometers. As a result, the gaseous target length as seen by the spectrometers could not be accurately defined, and the rejection of events originating from the end-caps was

$x$	$Q^2$ (GeV/c) <sup>2</sup>	$W^2$ (GeV/c <sup>2</sup> ) <sup>2</sup>	$\sigma_h/\sigma_t$	$\Delta_{\text{stat}}$	$\Delta_{\text{ptp}}$	$\Delta_{\text{syst}}$	$\Delta_{\text{tot}}$
0.195	2.73	12.2	1.112	0.003	0.005	0.008	0.010
0.225	3.15	11.7	1.124	0.003	0.004	0.008	0.010
0.255	3.57	11.3	1.141	0.004	0.004	0.008	0.010
0.285	3.99	10.9	1.160	0.005	0.005	0.008	0.011
0.315	4.41	10.5	1.154	0.005	0.004	0.008	0.011
0.345	4.83	10.1	1.171	0.006	0.005	0.008	0.011
0.375	5.25	9.63	1.177	0.008	0.006	0.008	0.013
0.405	5.67	9.21	1.219	0.009	0.004	0.009	0.014
0.435	6.09	8.79	1.206	0.010	0.005	0.009	0.014
0.465	6.51	8.37	1.226	0.010	0.004	0.009	0.014
0.495	6.93	7.95	1.235	0.010	0.004	0.009	0.014
0.525	7.35	7.53	1.260	0.011	0.004	0.009	0.015
0.555	7.77	7.11	1.267	0.011	0.004	0.009	0.015
0.585	8.19	6.69	1.268	0.012	0.004	0.009	0.016
0.615	8.61	6.27	1.268	0.013	0.004	0.009	0.016
0.645	9.03	5.85	1.292	0.013	0.004	0.009	0.017
0.675	9.45	5.43	1.289	0.014	0.004	0.009	0.018
0.705	9.87	5.01	1.309	0.014	0.004	0.009	0.017
0.735	10.3	4.59	1.302	0.013	0.004	0.009	0.017
0.765	10.7	4.17	1.316	0.014	0.004	0.009	0.017
0.795	11.1	3.75	1.312	0.015	0.004	0.009	0.018
0.825	11.9	3.40	1.301	0.017	0.004	0.009	0.020

TABLE II: The helion to triton DIS cross section ratio (after normalization, see text) at the  $x$ ,  $Q^2$ , and  $W^2$  kinematics of MARATHON. Listed also are the statistical (stat), point-to-point (ptp) and overall/scale systematic (syst) components of the total (tot) error. The latter is the quadrature of the three components.

accomplished by using a software “target position reconstruction cut”. This cut rejected events which were reconstructed by the spectrometers to originate from a position in the target cell close to the end-caps. Typically, events with a reconstructed position within a range of 2 cm from the end-caps were eliminated, resulting in an average effective target length,  $L_t$ , of 21 cm. Only events with one track in the drift chambers that was clearly within the well-established angular and momentum acceptance limits of the spectrometers were included in the electron data sample. Events with two or more tracks were dominated by those passing through the edges of the exit of the Al vacuum pipe in the spectrometers.

All events properly identified as electrons originating from the gas inside each target cell were binned by Bjorken  $x$ , resulting in the formation of an electron yield,  $Y(x)$ , defined as:

$$Y(x) = \frac{N_{e'}}{N_e \rho_t L_t} C_{\text{cor}}, \quad (3)$$

where  $N_{e'}$  is the number of scattered electrons (events found within the spectrometer acceptance limits that passed the Čerenkov, calorimeter and target “cuts”),  $N_e$  is the number of incident beam electrons,  $\rho_t$  is the density of the gas target,  $L_t$  is the selected target length, and  $C_{\text{cor}} = C_{\text{det}} C_{\text{cdt}} C_{\text{den}} C_{\text{tec}} C_{\text{psp}} C_{\text{rad}} C_{\text{cde}} C_{\text{bin}} C_{\text{dth}}$ . Here,  $C_{\text{det}}$  is the correction for trigger and detector inefficiency,  $C_{\text{cdt}}$  is the computer dead-time correction (1.001

$x$	$\mathcal{R}_{ht}$	$\Delta\mathcal{R}_{ht}$	$F_2^n/F_2^p$	$\Delta_{stat}$	$\Delta_{ptp}$	$\Delta_{syst}$	$\Delta_{tot}$
0.195	0.9989	0.0009	0.724	0.005	0.011	0.016	0.020
0.225	0.9990	0.0009	0.701	0.006	0.008	0.016	0.019
0.255	0.9991	0.0009	0.668	0.008	0.008	0.015	0.019
0.285	0.9993	0.0008	0.635	0.008	0.009	0.014	0.019
0.315	0.9997	0.0009	0.647	0.010	0.008	0.015	0.019
0.345	1.0003	0.0008	0.618	0.010	0.008	0.014	0.019
0.375	1.0010	0.0008	0.610	0.013	0.010	0.014	0.021
0.405	1.0019	0.0008	0.547	0.014	0.006	0.013	0.020
0.435	1.0029	0.0007	0.567	0.015	0.007	0.013	0.021
0.465	1.0039	0.0007	0.540	0.015	0.006	0.013	0.020
0.495	1.0049	0.0007	0.528	0.014	0.006	0.012	0.020
0.525	1.0058	0.0007	0.496	0.015	0.006	0.012	0.020
0.555	1.0067	0.0007	0.489	0.015	0.006	0.012	0.020
0.585	1.0074	0.0008	0.489	0.016	0.006	0.012	0.020
0.615	1.0081	0.0009	0.489	0.016	0.005	0.012	0.021
0.645	1.0087	0.0010	0.461	0.016	0.006	0.011	0.020
0.675	1.0093	0.0013	0.466	0.018	0.006	0.011	0.022
0.705	1.0098	0.0017	0.442	0.016	0.005	0.011	0.020
0.735	1.0104	0.0020	0.451	0.016	0.005	0.011	0.020
0.765	1.0111	0.0024	0.436	0.016	0.006	0.011	0.020
0.795	1.0118	0.0030	0.441	0.017	0.006	0.011	0.022
0.825	1.0125	0.0043	0.455	0.020	0.009	0.011	0.024

TABLE III: The  $F_2^n/F_2^p$  ratio for the MARATHON  $x$  kinematics. Listed also are the ratio's statistical (stat), point-to-point (ptp), and overall/scale (syst) components of the total (tot) error. The latter is the quadrature of the three components. Also listed are the values for the  $\mathcal{R}_{ht}$  super-ratio and their uncertainties used in the  $F_2$  ratio extraction (see text).

to 1.065),  $C_{den}$  is a correction to the target density due to beam heating effects (1.066 to 1.125),  $C_{tec}$  is a correction for falsely-reconstructed events originating from the end-caps (0.973 to 0.998),  $C_{psp}$  is a correction for events originating from pair symmetric processes (0.986 to 0.999),  $C_{rad}$  is a correction for radiative effects (0.826 to 1.173),  $C_{cde}$  is a correction for Coulomb distortion effects (0.997 to 1.000),  $C_{bin}$  is a bin-centering correction (0.995 to 1.001), and  $C_{dth}$  is a correction for the beta decay of tritons to helions, applicable only to the tritium yield [0.997 (0.989) at the beginning (end) of the experiment]. A cross section model by Kulagin and Petti (K-P), based on the works of Refs. [40–42], was adopted [43] for the bin-centering correction, and the Coulomb correction (which used the  $Q^2$ -effective approximation [44]).

When forming ratios of electron yields from different targets, which are equivalent to cross section ratios, the effective gas target length  $L_t$  (18.0–22.5 cm) and the correction  $C_{det}$  cancel out. In general, the corrections to the *ratios* from each effect become minimal, and in some cases, so do the associated systematic uncertainties. For example, the radiative effect correction, ranges from 0.997 (at the highest  $x$ ) to 1.015 (at the lowest  $x$ ) for the  $h/t$  cross section ratio. The dominant point-to-point systematic uncertainties for the yield ratios are those from the beam-heating gas target density changes [ $\pm(0.1\%-0.5\%)$ ], the radiative correction [ $\pm(0.25\%-0.45\%)$ ], and the choice of spectrometer acceptance limits ( $\pm 0.2\%$ ). The total point-to-point uncertainty ranged from  $\pm 0.4\%$  to  $\pm 1.0\%$  for the  $d/p$  cross section ratio, and  $\pm 0.3\%$  to

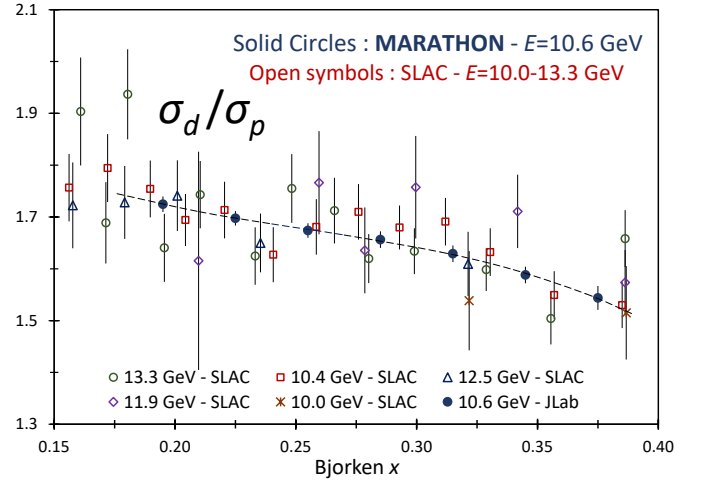


FIG. 1: The ratio of the DIS cross sections of deuteron and proton plotted versus the Bjorken  $x$  from the JLab Hall A MARATHON experiment. Also shown are seminal SLAC data [45] in the same kinematic region as MARATHON (see text). The dashed curve is a fit to the MARATHON data. The JLab error bars include all uncertainties added in quadrature. The SLAC error bars do not include an overall normalization uncertainty of  $\pm 1.3\%$ .

$\pm 0.5\%$  for the  $h/t$  ratio. Details on the determination of the yields, and all associated corrections and uncertainties, can be found in Refs. [35–39].

The experiment also collected DIS data for the proton and deuteron ( $d$ ) over the  $x$  range from 0.19 to 0.37 for the purpose of finding the  $F_2^n/F_2^p$  ratio in the vicinity of  $x = 0.3$ , where it is known that nuclear corrections are minimal [40, 42], and comparing it with the  $F_2^n/F_2^p$  ratio found using DIS by the triton and helion. The measured values of the  $\sigma_d/\sigma_p$  ratio are given in Table I. In addition to the  $x$  and  $Q^2$  for each kinematic setting, the values of the square of the invariant mass of the final hadronic state,  $W^2 = M^2 + 2M\nu - Q^2$ , are also given in Table I. The  $\sigma_d/\sigma_p = F_2^d/F_2^p$  values, plotted in Figure 1, are compared to measurements from the seminal SLAC E49b and E87 experiments [45] taken with similar beam energies. It is evident from Fig. 1 that the JLab and SLAC data are in excellent agreement. Given the ratio  $\mathcal{R}_d = F_2^d/(F_2^p + F_2^n)$ , the  $F_2^n/F_2^p$  ratio is calculated as  $F_2^n/F_2^p = (F_2^d/F_2^p)/\mathcal{R}_d - 1$  [26, 41]. The  $\mathcal{R}_d$  ratio used in the MARATHON  $F_2^d/F_2^p$  data analysis is from the model by Kulagin and Petti based on Refs. [40, 41]. The results of this model are, in the vicinity of  $x = 0.3$ , in excellent agreement with determinations using data from the JLab BoNuS [46] and SLAC E139 [19] experiments, and a theoretical calculation based on a study of data from DIS off nuclei with mass number  $A \geq 4$  [42].

The focus of MARATHON was to study DIS from helion and triton in order to extract the  $F_2^n/F_2^p$  ratio in the range  $0.19 < x < 0.83$  using the measured  $\sigma_h/\sigma_t = F_2^h/F_2^t$  ratio and model-calculated values of the super-ratio  $\mathcal{R}_{ht}$ . The values used for  $\mathcal{R}_{ht}$  come from the theoretical model by Kulagin and Petti [41, 42], which

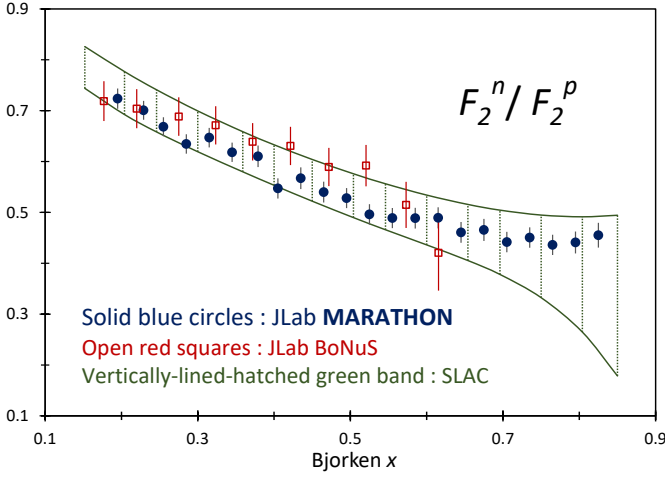


FIG. 2: The  $F_2^n/F_2^p$  ratio plotted versus the Bjorken  $x$  from the JLab MARATHON experiment. Also shown are JLab Hall B BoNuS data [53], and a band based on the fit of the SLAC data as provided in Ref. [45], for the MARATHON kinematics [ $Q^2 = 14 \cdot x$  (GeV/c) $^2$ ] (see text). All three experimental data sets include point to point and normalization systematic uncertainties.

provides a global description of the EMC effect for all known targets (for a review see Ref. [47]). The K-P model includes a number of nuclear effects out of which the major correction for the relevant kinematics comes from the smearing effect with the nuclear energy-momentum distribution, described in terms of the nuclear spectral function, together with an off-shell correction to the bound nucleon  $F_2$  [42]. The underlying proton and neutron structure functions come from the global QCD analysis of Ref. [48], which was performed up to NNLO approximation in the strong coupling constant including target mass corrections [49] as well as those due to higher-twist effects. For the spectral functions of the  $^3\text{H}$  and  $^3\text{He}$  nuclei, the results of Ref. [26] have been used. In order to evaluate theoretical uncertainties, the  $^3\text{He}$  spectral function of Ref. [50] was used. Reasonable variations of the high-momentum part of momentum distribution in  $^3\text{H}$  and  $^3\text{He}$  were considered, and uncertainties in the off-shell correction of Ref. [42], as well as in the nucleon structure functions, were accounted for. The maximum resulting uncertainty in  $\mathcal{R}_{ht}$  is estimated to be up to  $\pm 0.4\%$  (at  $x = 0.8$ ), contributing minimally to the total uncertainty in the final  $F_2^n/F_2^p$  values. The K-P calculations were performed prior to the analysis of the MARATHON data.

The comparison of  $F_2^n/F_2^p$  as extracted from  $\sigma_h/\sigma_t$  and  $\sigma_d/\sigma_p$  was done at the  $x$  value of 0.31, where it is widely accepted that nuclear corrections contribute negligibly to EMC-type ratios like  $\mathcal{R}_d$  and  $\mathcal{R}_{ht}$ , as  $\sigma_A/A = \sigma_d/2$  [51]. The K-P models used, predicted a value of 1.000 at  $x = 0.31$  for both  $\mathcal{R}_{ht}$  and  $\mathcal{R}_d$  with uncertainties of  $\pm 0.1\%$  and  $\pm 0.2\%$ , respectively. A recent work by Segarra *et al.* [52] found  $\mathcal{R}_{ht}(x = 0.31) = 1.001$ , with a similar uncertainty. This work is based on a global analysis of nuclear DIS data where the EMC effect is accounted for by

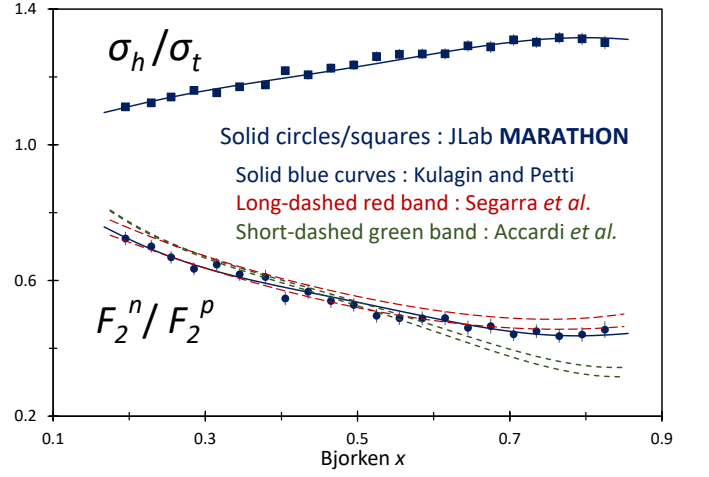


FIG. 3: The DIS  $\sigma_h/\sigma_t$  and the  $F_2^n/F_2^p$  ratios from the MARATHON experiment, plotted versus the Bjorken  $x$ , compared to the theoretical predictions of Kulagin and Petti. The  $F_2^n/F_2^p$  data are also compared to a CJ Collaboration prediction [56] (short-dashed band), and a recent extraction by Segarra *et al.* [52] (long-dashed band) (see text). The error bars include overall systematic uncertainties. All curves correspond to the MARATHON kinematics [ $Q^2 = 14 \cdot x$  (GeV/c) $^2$ ].

a universal modification of nucleons through short-range correlations. The values of  $\sigma_d/\sigma_p$  and  $\sigma_h/\sigma_t$  at  $x = 0.31$  were determined by weighted fits to the MARATHON data, which included statistical and point-to-point uncertainties added in quadrature. In order to match the  $F_2^n/F_2^p$  values found using the two different sets of nuclei, the  $\sigma_h/\sigma_t$  ratio at  $x = 0.31$  had to be normalized by a multiplicative factor of  $1.025 \pm 0.007$ . Consequently, all values of  $\sigma_h/\sigma_t$  reported in this work have been normalized upwards by 2.5%.

The normalized  $\sigma_h/\sigma_t$  values are given in Table II along with statistical, point-to-point, overall/scale, and total uncertainties. The  $x$ ,  $Q^2$  and  $W^2$  values of each kinematic setting are also given in Table II. The  $F_2^n/F_2^p$  values are given in Table III along with statistical, point-to-point, overall/scale, and total uncertainties. Shown also in Table III are the  $\mathcal{R}_{ht}$  super-ratio values used to find  $F_2^n/F_2^p$ . The  $\mathcal{R}_{ht}$  uncertainty was incorporated in quadrature with the point-to-point  $F_2^n/F_2^p$  uncertainty. Figure 2 shows the MARATHON results for the  $F_2^n/F_2^p$  ratio, along with data from the JLab Hall B BoNuS experiment [53] for  $W^2 > 3.25$  (GeV/c) $^2$ , evolved to the  $Q^2$  of MARATHON [16], and the results from early SLAC measurements with  $W^2 > 3.30$  (GeV/c) $^2$  [10, 45]. All results include statistical and point-to-point uncertainties, as well as overall (scale) uncertainties. The SLAC results are presented as a band, the width of which at high  $x$  is dominated primarily by uncertainties due the choice of the N-N potential used for the evaluation of the deuteron wave function [16, 21, 22]. The MARATHON data are in good agreement with the BoNuS data, and fall well within the SLAC results band. The highest- $x$  points are consistent with the  $F_2^n/F_2^p$  ratio tending to a value between 0.4 and 0.5 at  $x = 1$ . This is consistent with

the predictions of perturbative QCD and quark counting rules (for which this ratio is  $3/7$  at  $x = 1$ ), and with a recent prediction [54] that treats strong interactions using the Dyson-Schwinger equations, where diquark correlations in the nucleons are consequences of dynamical chiral symmetry breaking (for which the nucleon  $F_2$  ratio lies, at  $x = 1$ , between 0.4 and 0.5). It is also consistent with a covariant quark-diquark model which also predicts that the  $F_2$  ratio should be  $3/7$  at  $x = 1$  [55].

The MARATHON  $F_2^n/F_2^p$  ratio values are in excellent agreement with those predicted by Kulagin and Petti based on nucleon structure functions from the global QCD analysis of Refs. [40, 48], as quantified by a  $\chi^2$  per degree of freedom of 0.8. The MARATHON  $F_2^n/F_2^p$  results are compared to the K-P prediction in Figure 3. Shown also in the Figure are the  $\sigma_h/\sigma_t$  MARATHON values compared with the K-P prediction, which uses the nucleon structure functions of Refs. [40, 48] and the  $A = 3$  spectral functions of Ref. [26]. Also shown in Figure 3 is a recent nuclear DIS determination by Segarra *et al.* [52], and the most recent calculation for  $F_2^n/F_2^p$  by the CTEQ-JLab (CJ) Collaboration [56], evolved to the  $Q^2$  of MARATHON [52].

The precision of the MARATHON data is expected to constrain theoretical models of the few body nuclear structure functions, and to be used in algorithms which fit [40, 56, 57] hadronic data to determine the essentially unknown  $(u + \bar{u})/(d + \bar{d})$  ratio at large Bjorken  $x$ . It

should be noted that additional high-quality data on the nucleon  $F_2$  ratio are expected from the extension [58] of the original BoNuS experiment [53] using semi-inclusive electron-deuteron scattering with a 10.4 GeV beam. In addition, MARATHON will disseminate, in a separate communication, results on the EMC effect of  $^3\text{H}$  and  $^3\text{He}$ , incorporating a full set of DIS data taken with the deuterium target over the full  $x$ -range of the experiment.

We acknowledge the outstanding support of the staff of the Accelerator Division and Hall A Facility of JLab, and work of the staff of the Savannah River Tritium Enterprises and the JLab Target Group. We thank Dr. M. E. Christy for useful discussions on the optical properties of the HRS systems. We are grateful to Dr. W. Melnitchouk for his contributions to the development of the MARATHON proposal, and to Dr. A. W. Thomas for many valuable discussions on and support of the MARATHON project since its inception. This material is based upon work supported by the U.S. Department of Energy (DOE), Office of Science, Office of Nuclear Physics under contracts DE-AC05-06OR23177 and DE-AC02-06CH11357. This work was also supported by DOE contract DE-AC02-05CH11231, DOE award DE-SC0016577, National Science Foundation awards NSF-PHY-1405814 and NSF-PHY-1714809, the Kent State University Research Council, the Pazy Foundation and the Israeli Science Foundation under grants 136/12 and 1334/16, and the Italian Institute of Nuclear Physics.

- 
- [1] 1990 Nobel Lectures in Physics: J. I. Friedman, *Rev. Mod. Phys.* **63**, 615 (1991); H. W. Kendall, *Rev. Mod. Phys.* **63**, 597 (1991); R. E. Taylor, *Rev. Mod. Phys.* **63**, 573 (1991).
  - [2] J. I. Friedman and H. W. Kendall, *Annu. Rev. Nucl. Sci.* **22**, 203 (1972); and references therein.
  - [3] D. H. Perkins, *Rep. Prog. Phys.* **40**, 409 (1977).
  - [4] F. E. Close, *An Introduction to Quarks and Partons*, Academic Press, London (1979).
  - [5] F. J. Yndurain, *Quantum Chromodynamics*, Springer-Verlag, Berlin (1983); T. Muta, *Foundations of Quantum Chromodynamics*, World Scientific, Singapore (1987).
  - [6] D. F. Geesaman, K. Saito, and A. W. Thomas, *Annu. Rev. Nucl. Part. Science* **45**, 337 (1995); L. H. Tao *et al.*, *Z. Phys.* **C70**, 387 (1996).
  - [7] J. D. Bjorken, *Phys. Rev.* **179**, 1547 (1969); J. D. Bjorken and E. A. Paschos, *Phys. Rev.* **185**, 1975 (1969).
  - [8] R. P. Feynman, *Phys. Rev. Lett.* **23**, 1415 (1969).
  - [9] O. Nachtmann, *Nucl. Phys.* **B38**, 397 (1972).
  - [10] A. Bodek, M. Breidenbach, D. L. Dubin, J. E. Elias, J. I. Friedman, H. W. Kendall, J. S. Poucher, E. M. Riordan, M. R. Sogard, and D. H. Coward (SLAC-E49b), *Phys. Rev. Lett.* **30**, 1087 (1973); J. S. Poucher *et al.* (SLAC-E49a), *Phys. Rev. Lett.* **32**, 118 (1974).
  - [11] F. E. Close, *Phys. Lett.* **B43**, 422 (1973).
  - [12] R. P. Feynman, in *Proceedings of 3rd International Conference of High Energy Collisions*, Gordon and Breach, 1970; R. Carlitz, *Phys. Lett.* **B58**, 345 (1975).
  - [13] N. Isgur, *Phys. Rev.* **D59**, 034013 (1999).
  - [14] G. R. Farrar and D. R. Jackson, *Phys. Rev. Lett.* **35**, 1416 (1975).
  - [15] S. J. Brodsky, M. Burkardt, and I. Schmidt, *Nucl. Phys.* **B441**, 197 (1995).
  - [16] L. W. Whitlow, E. M. Riordan, S. Dasu, S. Rock, and A. Bodek, *Phys. Lett.* **B282**, 475 (1992); and Ref. [9] therein.
  - [17] L. L. Frankfurt and M. I. Strikman, *Phys. Rep.* **160**, 235 (1988).
  - [18] J. J. Aubert *et al.*, *Phys. Lett.* **B123**, 275 (1983).
  - [19] J. Gomez *et al.*, *Phys. Rev.* **D49**, 4348 (1994).
  - [20] W. Melnitchouk and A. W. Thomas, *Phys. Lett.* **B377**, 11 (1996).
  - [21] A. Accardi, W. Melnitchouk, J. F. Owens, M. E. Christy, C. E. Keppel, L. Zhu, and J. G. Morfin, *Phys. Rev.* **D84**, 014008 (2011).
  - [22] J. Arrington, J. G. Rubin, and W. Melnitchouk, *Phys. Rev. Lett.* **108**, 252001 (2012).
  - [23] I. R. Afnan, F. Bissey, J. Gomez, A. T. Katramatou, W. Melnitchouk, G. G. Petratos and A. W. Thomas, *Phys. Lett.* **B493**, 36 (2000).
  - [24] I. R. Afnan, F. Bissey, J. Gomez, A. T. Katramatou, S. Liuti, W. Melnitchouk, G. G. Petratos and A. W. Thomas, *Phys. Rev.* **C68**, 035201 (2003).
  - [25] G. G. Petratos, J. Gomez, A. T. Katramatou, and W. Melnitchouk, in *Proceedings of Workshop on Experiments with Tritium at JLab*, Jefferson Lab, Newport News, Virginia, September 1999.
  - [26] E. Pace, G. Salmè, S. Scopetta and A. Kievsky, *Phys.*



- Rev. **C64**, 055203 (2001).
- [27] M. M. Sargsian, S. Simula and M. I. Strikman, Phys. Rev. **C66**, 024001 (2002).
- [28] G. G. Petratos *et al.*, JLab PR12-10-103 **MARATHON** Proposal: **MeAsurement of the  $F_2^n/F_2^p$ ,  $d/u$  RAtios and  $A=3$  EMC Effect in Deep Inelastic Electron Scattering Off the TTritium and Helium MirrOr Nuclei**, 2010.
- [29] J. Alcorn *et al.*, Nucl. Instrum. Methods Phys. Res. **A522**, 294 (2004).
- [30] R. J. Holt *et al.*, *Conceptual Design of a Tritium Gas Target for JLab* (JLab report), May 2010; S. N. Santiesteban *et al.*, Nucl. Instrum. Methods Phys. Res. **A940**, 351 (2019).
- [31] G. Garberoglio, P. Jankowski, K. Szalewicz, and A. Hurvey, J. Chem. Phys. **137**, 154308 (2012); P. Czachorowski, M. Przybytek, M. Lesiuk, M. Puchalski, and B. Jerioski, Phys. Rev. **A102**, 042810 (2020); and references therein.
- [32] H. Collard *et al.*, Phys. Rev. **138**, 57 (1965).
- [33] D. H. Beck *et al.*, Nucl. Instrum. Methods Phys. Res. **A277**, 323 (1989).
- [34] J. Bane, Ph.D. Thesis, University of Tennessee, 2019.
- [35] T. Hague, Ph.D. Thesis, Kent State University, 2020.
- [36] T. Kutz, Ph.D. Thesis, Stony Brook University, 2019.
- [37] H. Liu, Ph.D. Thesis, Columbia University, 2020.
- [38] M. Nycz, Ph.D. Thesis, Kent State University, 2020.
- [39] T. Su, Ph.D. Thesis, Kent State University, 2020.
- [40] S. I. Alekhin, S. A. Kulagin, and R. Petti, Phys. Rev. **D96**, 054005 (2017).
- [41] S. A. Kulagin and R. Petti, Phys. Rev. **C82**, 054614 (2010).
- [42] S. A. Kulagin and R. Petti, Nucl. Phys. **A765**, 126 (2006).
- [43] Sergey Kulagin and Roberto Petti, private communication, 2018.
- [44] Herbert Uberall, *Electron Scattering from Complex Nuclei*, Academic Press (1971).
- [45] A. Bodek *et al.* (SLAC-E49/E87), Phys. Rev. **D20**, 1471 (1979).
- [46] K. A. Griffioen *et al.*, Phys. Rev. **C92**, 015211 (2015).
- [47] S. A. Kulagin, EPJ Web Conf. **138**, 01006 (2017).
- [48] S. Alekhin, S. A. Kulagin and R. Petti, AIP Conf. Proc. **967**, 215 (2007).
- [49] H. Georgi, H. D. Politzer, Phys. Rev. **D14**, 1829 (1976).
- [50] R. W. Schulze and P. U. Sauer, Phys. Rev. **C48**, 38 (1993).
- [51] L. B. Weinstein, E. Piasetzky, D. W. Higinbotham, J. Gomez, O. Hen, and R. Shneor, Phys. Rev. Lett. **106**, 052301 (2011).
- [52] E. P. Segarra, A. Schmidt, T. Kutz, D. W. Higinbotham, E. Piasetzky, M. Strikman, L. B. Weinstein, and O. Hen, Phys. Rev. Lett. **124**, 092002 (2020).
- [53] S. Tkachenko *et al.*, Phys. Rev. **C89**, 045206 (2014).
- [54] C. D. Roberts, R. J. Holt, and S. M. Schmidt, Phys. Lett. **B727**, 249 (2013).
- [55] I. C. Cloët, W. Bentz, and A. W. Thomas, Phys. Lett. **B621**, 246 (2005).
- [56] A. Accardi, L. T. Brady, W. Melnitchouk, J. F. Owens, and N. Sato, Phys. Rev. **D93**, 114017 (2016).
- [57] S. Dulat, T. J. Hou, J. Gao, M. Guzzi, J. Huston, P. Nadolsky, J. Pumplin, C. Schmidt, D. Stamp, and C.-P. Yuan, Phys. Rev. **D93**, 033006 (2016).
- [58] S. Bueltmann *et al.* (The JLab BoNuS Collaboration), *The Structure of the Free Neutron at Large  $x$ -Bjorken*, JLab 12 GeV Proposal PR12-10-102 (2010).